Talanta 82 (2010) 892–898

Contents lists available at ScienceDirect

Talanta

journal homepage: www.elsevier.com/locate/talanta

2D spatiotemporal visualization system of expired gaseous ethanol after oral administration for real-time illustrated analysis of alcohol metabolism

Xin Wang[a], Eri Ando[b], Daishi Takahashi[b], Takahiro Arakawa[b], Hiroyuki Kudo[b], Hirokazu Saito[c], Kohji Mitsubayashi[a,b,*]

[a] Graduate School of Medical and Dental Sciences, Tokyo Medical and Dental University, 1-5-45 Yushima, Bunnkyo-ku, Tokyo 113-8510, Japan
[b] Department of Biomedical Devices and Instrumentation, Institute of Biomaterials and Bioengineering, Tokyo Medical and Dental University, 2-3-10 Kanda-Surugadai, Chiyoda-ku, Tokyo 101-0062, Japan
[c] Department of Mechanical Engineering, Tokyo National College of Technology, 1220-2 Kunagida-machi, Hachioji-shi, Tokyo 193-0997, Japan

ARTICLE INFO

Article history:
Received 8 March 2010
Received in revised form 21 April 2010
Accepted 21 April 2010
Available online 29 April 2010

Keywords:
Spatiotemporal visualization system
Expired gaseous ethanol
Alcohol metabolism
Chemiluminescence
Oral alcohol administration
Luminol solution

ABSTRACT

A novel 2-dimensional spatiotemporal visualization system of expired gaseous ethanol after oral administration for real-time illustrated analysis of alcohol metabolism has been developed, which employed a low level light CCD camera to detect chemiluminescence (CL) generated by catalytic reactions of standard gaseous ethanol and expired gaseous ethanol after oral administration. First, the optimization of the substrates for visualization and the concentration of luminol solution for CL were investigated. The cotton mesh and 5.0 mmol L^{-1} luminol solution were selected for further investigations and this system is useful for 0.1–20.0 mmol L^{-1} of H_2O_2 solution. Then, the effect of pH condition of Tris–HCl buffer solution was also evaluated with CL intensity and under the Tris–HCl buffer solution pH 10.1, a wide calibration range of standard gaseous ethanol (30–400 ppm) was obtained. Finally, expired air of 5 healthy volunteers after oral administration was measured at 15, 30, 45, 60, 75, 90, 105 and 120 min after oral administration, and this system showed a good sensitivity on expired gaseous ethanol for alcohol metabolism. The peaks of expired gaseous ethanol concentration appeared within 30 min after oral administration. During the 30 min after oral administration, the time variation profile based on mean values showed the absorption and distribution function, and the values onward showed the elimination function. The absorption and distribution of expired gaseous ethanol in 5 healthy volunteers following first-order absorption process were faster than the elimination process, which proves efficacious of this system for described alcohol metabolism in healthy volunteers. This system is expected to be used as a non-invasive method to detect VOCs as well as several other drugs [1] in expired air for clinical purpose.

1. Introduction

In recent 2-decade, the medical monitoring technologies and diagnostics focused on blood and urine analysis have developed. Relatively, the bulk matrix of breath, containing large amounts of N_2, O_2, CO_2 and H_2O, contains over 1000 trace amounts of the VOCs [2–5]. The content may be generated in the body or may be absorbed from the environment as contaminants. The bulk matrix and trace VOCs exchange between the blood and alveolar air at the blood–gas interface in the lung.

Meanwhile, alcohol is a central nervous system depressant and it is the central nervous system. The degree to which the central nervous system function impaired is directly proportional to the concentration of alcohol in the blood. In a fasting individual, it is generally agreed that 20–25% of a dose of alcohol is absorbed from the stomach and 75–80% is absorbed from the small intestine. The liver is responsible for the elimination of 95% of ingested alcohol as well as other drugs from the body. The remainder of the alcohol is eliminated through excretion of alcohol in breath, urine, sweat, feces, milk and saliva.

Many breath alcohol analyzers assume a constant blood ethanol concentration/breath ethanol concentration ratio of 2100 for this conversion [6]. The measurement of expired gaseous ethanol could monitor the blood ethanol concentration non-invasive. Pharmacokinetic models for in vivo ethanol elimination have been calculated from the intravenous experiments by assuming that blood ethanol concentration equals [7].

* Corresponding author at: Department of Biomedical Devices and Instrumentation, Institute of Biomaterials and Bioengineering, Tokyo Medical and Dental University, 2-3-10 Kannda-Surugadai, Chiyoda-ku, Tokyo 101-0062, Japan.
Tel.: +81 3 5280 8091; fax: +81 3 5280 8094.
E-mail address: m.bdi@tmd.ac.jp (K. Mitsubayashi).

0039-9140/$ – see front matter © 2010 Elsevier B.V. All rights reserved.
doi:10.1016/j.talanta.2010.04.048

Furthermore, analysis of the expired air is a non-invasive method for clinical purposes and the measurement of particular compounds in expired air would provide concerning disease states [8,9]. Expired air analysis has been used for 50 years since it was developed in the 1950s [10]. Modern expired air analysis started in the 1970s, using gas chromatography (GC), identified more than 200 components in human expired air [2]. And gas chromatography and mass spectrometry analysis (GC/MS analysis) was commonly used for expired air analysis by analyzing the component in expired air. Resent years, many technologies have been developed for sensor employing enzymatic reaction, such as bioelectronic sniffers for ethanol and acetaldehyde [11], bio-sniffer stick for gaseous formaldehyde [12] and A NADH-dependent fiberoptic biosensor for ethanol determination [13–16]. And as a result of extensive studies, a few breath markers have been discovered and successfully used in the diagnosis of disease. As such [$C^{13,14}$] urea breath test in the diagnosis of Helicobacter pylori infection [17,18], and the NO expired air analysis in the diagnosis of airway infection [2,19] have been successfully used as diagnostic method in clinical analysis. However the measurement by GC or GC/MS, a large volume of expired air (~2 L) is needed and the liquid nitrogen or liquid argon is used for cryogenic preconcentration, which are necessary to sample analysis [20,21]. For this reason, a rapid, simple technology of expired air analysis for gaseous ethanol is required.

Otherwise, CL analyzer has been successfully used for NO expired air analysis directly without preconcentration, because of CL is a technique showing high sensitivity [22,23]. So a technology coupled with CL might be successfully used for expired air in clinical evaluation and application. Among the CL measurement, HRP–luminol–H_2O_2 system is the most popular technology and has been employed in many assays, such as estradiol in human serum [24], adenosine triphosphate detection in cancer cells [25], asulam [26], sulfamethoxypyridazine [27], total antioxidant activity [28].

Considering to the content mentioned above, the expired gaseous ethanol after oral administration was selected for predicting time trajectories for ethanol concentration, one of few specific expired air tests are available.

In this study, we fabricate a 2D visualization system of expired gaseous ethanol after oral administration for real-time illustrated analysis of alcohol metabolism. So we focus the attention on AOD, catalyzes low molecular weight alcohols by molecular oxygen (O_2) into aldehydes with the production of hydrogen peroxide (H_2O_2), which can be led to the HRP–luminol–H_2O_2 system for the CL analysis. We constructed the visualization system using the enzyme catalytic reaction for expired gaseous ethanol analysis after oral administration. This system is useful for the component in expired air not only spatial but also temporal analysis at real time. Prior to the measurement of expired gaseous ethanol, various concentrations of standard gaseous ethanol were adjusted and loaded onto the enzyme-immobilized substrate. The CL generated by the catalytic reaction of ethanol was detected and the image of CL was analyzed. The performance of this system has been evaluated, such as sensitivity, calibration, and compared with the performance of gas detector tube. We also discussed 2 kinds of substrates for the gaseous ethanol measurement by image analysis, optimized the concentration of luminol solution in the HRP–luminol–H_2O_2 system and optimized the pH condition of Tris–HCl buffer solution for gaseous ethanol measurement. Under the conditions optimized, the samples of expired air after oral administration were collected and analyzed by the 2D spatiotemporal visualization system. This system was confirmed for expired gaseous ethanol measurement and expected to be used as a non-invasive method to detect VOCs as well as several other drugs [1] in expired air for clinical purpose.

2. Experimental

2.1. Chemicals and apparatus

All solutions were prepared in deionized distilled water obtained from a Milli-Q purification system (Millipore Co., USA). Hydrophilic PTFE (H-PTFE) membrane filter (porosity: 80%, pore size: 0.2 μm, JGWP14225, Millipore Co., USA) and cotton mesh (cotton 100%, interval size: 1 mm, Pip-Fujimoto Co., Japan), were evaluated for the enzyme-immobilization in gaseous ethanol analysis.

A 15.0 mmol L^{-1} luminol (01253-60, Kanto Chemical Co., Inc., Japan) solution was prepared in Tris–HCl buffer solution (0.10 mmol L^{-1}, pH 9.0) for CL (generated by the catalytic reaction of H_2O_2) measurement. More diluted luminol solutions were prepared by suitable dilution of 15.0 mmol L^{-1} luminol solution with Tris–HCl buffer solution; these solutions were stable when stored in the dark. A 100.0 mmol L^{-1} hydrogen peroxide (H_2O_2, 18084-00, 31%, Kanto Chemical Co., Inc., Japan) solution was prepared by diluting in deionized distilled water. The concentration of H_2O_2 was determined by measuring the UV absorbance at 230 nm employing a UV/VIS Spectrophotometer (V-530, Jasco Corporation, Japan). More diluted solutions were prepared by suitable dilution of 100.0 mmol L^{-1} H_2O_2 solution freshly before use.

This system was constructed with a low light CCD camera (L3C95-05, pixel size: 15 μm × 35.5 μm, image format: 768 × 244 pixels, spectral range: 400–1060 nm, e2v technologies limited, United Kingdom), a HDD recorder (RD-XS32, Toshiba, Japan) and a video encoder (GV-MDVD3, I-O DATA, Japan). Data analyses were done by using Cosmos 32 software (Library Inc., Japan).

AOD (E.C.1.1.3.13, A2404-1KU, 10–40 units mg^{-1} protein, from *Pichia pastoris*, Sigma–Aldrich Co., USA) and HRP (E.C.1.11.1.7, 169-10791, 100 units mg^{-1}, Wako Pure Chemical Industries, Ltd., Japan), photo-crosslinkable poly (vinyl alcohol) containing stilbazolium groups (PVA-SbQ, type: SPH, 9C-10L, 10.4 wt%, Toyo Gosei Co., Ltd., Japan) were used for enzyme-immobilization.

2.2. CL and standard gaseous ethanol measurements

Prior to use in standard gaseous ethanol measurement, the characteristics of this system were analyzed with HRP-immobilized substrate for H_2O_2 measurement. HRP was dissolved in phosphate buffer solution (PB, 0.1 mmol L^{-1}, pH 7.5), and mixed with PVA-SbQ in a volume/weight ratio of 1:2. The enzyme/PVA-SbQ mixtures were coated onto the substrate, spread and cure for 3 h at 4 °C in dark. And then the substrate was treated with ultraviolet irradiation for 3 h. A HRP-immobilized substrate was obtained and stored at 4 °C before use. A comparison between the cotton mesh substrate and the H-PTFE substrate was carried out for further investigations of standard gaseous ethanol and expired gaseous ethanol measurement after oral administration.

The effect of concentration of luminol solution was investigated in the range of 1.0–15.0 mmol L^{-1} under experimental condition: [Tris–HCl buffer solution] = 0.1 mol L^{-1}; [H_2O_2] = 2.5 mmol L^{-1}. The concentration with the maximum CL was selected and used for further investigations.

The enzyme-immobilized substrate was rinsed with 3.0 ml of Tris–HCl buffer solution and dehydrated. And then the HRP-immobilized substrate was fixed in the dark box at a distance of 23.5 cm from the CCD camera, saturated with luminol solution. Schematic procedure of the measurement is shown in Fig. 1. Various concentrations of mist of H_2O_2 were sprayed onto the HRP-immobilized substrate, following the catalytic reaction (1), the CL generated on the substrate by spaying H_2O_2 solution

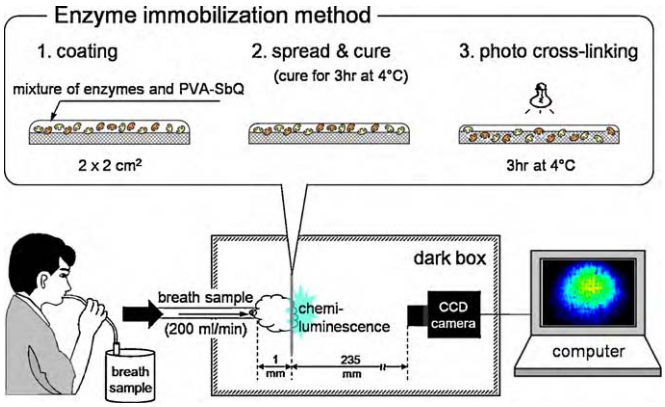

Fig. 1. Schematic procedure of the measurement for spatiotemporal visualization system. The system was constructed with an enzyme-immobilized substrate, a low light CCD camera, a HDD recorder, a video encoder and a computer.

was detected by the CCD camera and recorded for temporal changes.

$$2H_2O_2 + \text{luminol} + 2OH^- \xrightarrow{HRP} \text{3-aminophthalic acid} + 4N_2 + 4H_2O + h\lambda \quad (1)$$

After the measurement of CL, the AOD/HRP-immobilized substrate was prepared with PVA-SbQ in similar method to HRP-immobilization described above and used for gaseous ethanol measurement. A standard gaseous ethanol was supplied at a flow rate of 200 ml min^{-1} for 20 s from a gas generator (permeater, type: PD-1B-2, Gastec Co., Japan), which is employed as a standard gas generator for calibration purposes. The CL generated by loading gaseous ethanol was detected. Following the catalytic reaction ((2) and (3)), AOD catalyzes ethanol to acetaldehyde with the production of H_2O_2, which is one of the strongest oxidants to enhance the HRP–luminol–H_2O_2 system.

$$\text{ethanol} + O_2 \xrightarrow{AOD} \text{acetaldehyde} + H_2O_2 \quad (2)$$

$$2H_2O_2 + \text{luminol} + 2OH^- \xrightarrow{HRP} \text{3-aminophthalic acid} + 4N_2 + 4H_2O + h\lambda \quad (3)$$

2.3. Expired gaseous ethanol measurement after oral administration

For the measurement of gaseous ethanol in expired air, expired air samples after oral administration were collected and measured authorized by the Human Investigations Committee of Institute of Biomaterials and Bioengineering, Tokyo Medical and Dental University (authorization code: 0908-1, permitted since 14 September 2009), acting up to Declaration of Helsinki.

5 healthy volunteers, 3 males and 2 females, aged from 20 to 30 years old, have a body length between 150 and 170 cm and with body weights from 50 to 80 kg. All volunteers were asked to refrain from using alcohol, cigarettes, and other drugs that might alter alcohol metabolism for 3 days before experiment. After fasting for at least 4 h, each volunteer was given an alcohol drink (5% alcohol, 0.4 g/kg body weight) during a maximum time of 15 min. All volunteers remained in a chair for the duration of collecting expired air samples. Expired air samples were collected by having volunteers breathe at the end of expiration into a gas sampling bag (2 L, PVF, 9-834-02, 200 mm × 250 mm, AS ONE Co., Japan) though a 10.0 cm length-silicone tube (9-869-07, 4 mm × 6 mm, AS ONE Co., Japan), in 15-min intervals during 2 h.

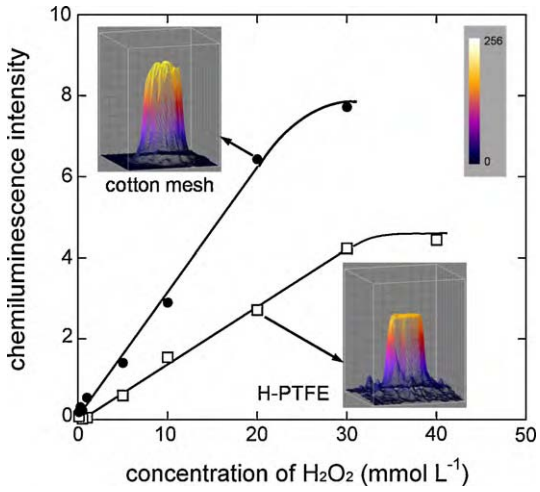

Fig. 2. Comparison calibration plots obtained on the cotton mesh (●) and the H-PTFE membrane (□). The CL intensities on the cotton mesh were higher than the ones on H-PTFE membrane, each of which showed a correlation coefficient of 0.997 (●) or 0.998 (□) with calibration range of 0.1–20.0 mmol L^{-1} (●) or 0.5–30.0 mmol L^{-1} (□). As shown in the images of 20.0 mmol L^{-1}, the intensity on the cotton mesh of the point, where H_2O_2 was sprayed, were higher than the one on H-PTFE membrane. About the 3D profiles in Figs. 2, 4 and 5, the *x* axis means the length of the mesh, *y* axis means the width of mesh and *z* axis means the intensity of CL.

The samples were warmed by a hot plate (HP-1S, AS ONE Co., Japan) to make sure that there is no moisture in the sample bag before use. The samples were drawn into a 60 ml syringe (polypropylene, Terumo Co., Japan), and then loaded onto the AOD/HRP-immobilized substrate under the same condition as the standard gaseous ethanol measurement described above. The syringe was rinsed with the sample before each measurement.

For the purpose of comparison, gas detector tubes (detection range: 50–2000 ppm, NO.112L, Gastec Co., Japan) were employed for the expired gaseous ethanol measurement. And gas detector tube is a highly stable detection reagent that is especially sensitive to alcohols in order to produce a distinct layer of color change.

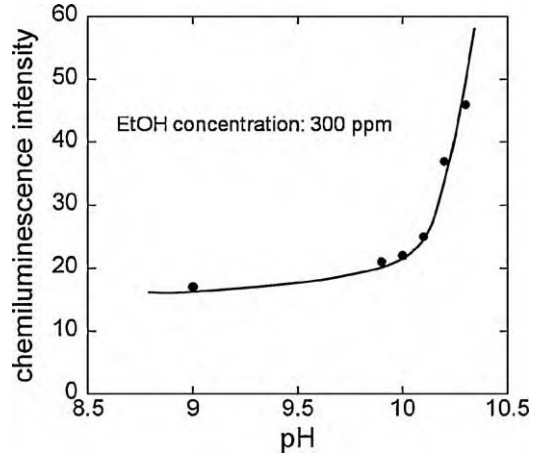

Fig. 3. Effect of pH of Tris–HCl buffer solution on CL intensity of standard gaseous ethanol (300 ppm). The pH of buffer solution was prepared with 0.10 mmol L^{-1} Tris–HCl, consisted of 5.0 mmol L^{-1} luminol. Although the highest CL intensity was observed at pH 10.3, the maximum intensities obtained at pH 10.3 and 10.2 were higher than 256, which could not be detected accurately by the CCD camera (8 bit). And in order to enhance the sensitivity of this system, Tris–HCl buffer solution (0.1 mol L^{-1}, pH 10.1) was selected and used for further investigations on standard gaseous ethanol and expired gaseous ethanol measurement.

3. Results and discussion

3.1. Evaluation of cotton mesh and H-PTFE membrane as enzyme-immobilized substrate

About the 3D profiles in Figs. 2, 4 and 5, the *x* axis means the length of the mesh, *y* axis means the width of mesh and *z* axis means the intensity of CL. Fig. 2 shows the comparison calibration plots obtained by employing the cotton mesh and the H-PTFE membrane. The CL intensity, calibration range and sensitivity were compared. Average CL intensities within the enzyme-immobilized substrates obtained by employing cotton mesh were higher than the ones employing H-PTFE membrane, which mainly because of the amount of HRP immobilized on the cotton mesh were more than on the H-PTFE. Images of 20.0 mmol L^{-1} are also shown in Fig. 2. The CL on the cotton mesh was detected stronger only at the point of H_2O_2 sprayed. But the CL on the H-PTFE membrane was weaker, spreading over the point of H_2O_2 solution sprayed.

And the calibration ranges for H_2O_2 solution were 0.1–20.0 mmol L^{-1} (cotton mesh) and 0.5–30.0 mmol L^{-1} (H-PTFE). The cotton mesh showed a good sensitivity in CL measurement than H-PTFE. Furthermore, gas current could easily pass through the enzyme-immobilized substrate; the mesh structure was suitable for the purpose of standard gaseous ethanol and expired gaseous ethanol measurement.

3.2. Optimization of the concentration of luminol and pH condition of Tris–HCl buffer solution

The experimental conditions were optimized by means of the univariate approach. For this reason, the effect of concentration of luminol solution on CL was investigated using Tris–HCl buffer

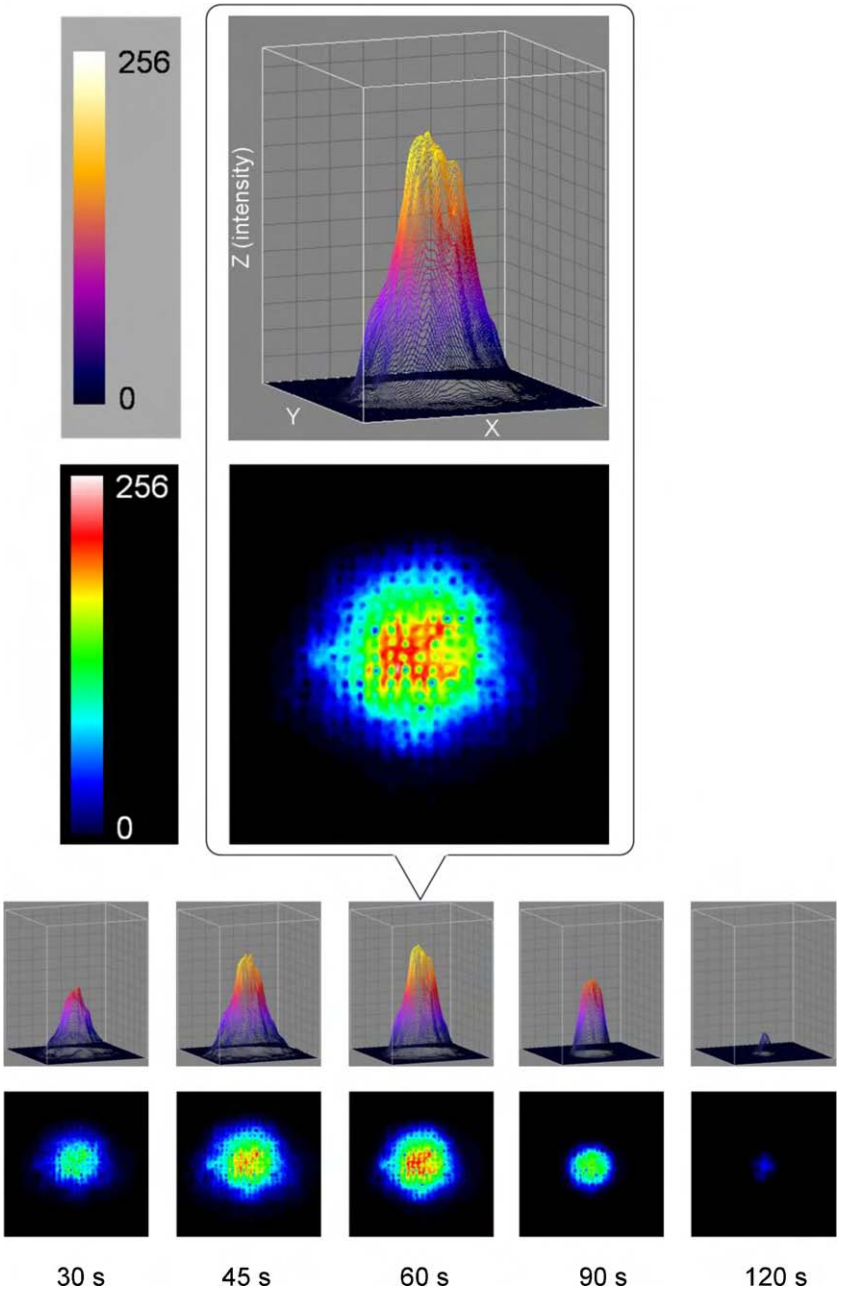

Fig. 4. The temporal changes of a standard gaseous ethanol (300 ppm) at 30, 45, 60, 90 and 120 s after its loading. The uppers were processed showing the different information of CL of gaseous ethanol in 3D profile. The lowers were the images of CL intensity, which processed showing the intensities in RGB.

solution (0.1 mol L^{-1}, pH 9.0) in the range of 1.0–15.0 mmol L^{-1}, the CL intensity reached a maximum at 5.0 mmol L^{-1} luminol solution (data not shown). Therefore, the 5.0 mmol L^{-1} luminol solution was selected for the further investigations.

The efficiency of HRP–luminol–H_2O_2 system was highly dependent on reaction pH [25]. And pH optimum around pH 8.5 for the majority of them was reported [29]. In our system, we employed AOD and HRP to detect the CL of ethanol, so the Tris–HCl buffer solution was not only the medium of AOD catalytic reaction but also the medium of the CL reaction catalyzed by HRP. Considering to luminol CL reaction, an alkaline medium would improve the sensitivity of this system (pH 10–11). However, the optimal pH value for AOD and HRP was pH 6–8 [30]. Furthermore, in order to obtain 5.0 mmol L^{-1} luminol solutions, an alkaline medium (pH > 8.5) was necessary. So the effect of medium pH was investigated for the purpose of gaseous ethanol measurement in the range pH 9.0–10.3, and pH 10.3 is almost the maximum pH in Tris–HCl buffer solution.

Considering to the range of expired gaseous ethanol concentration after oral administration, which was lower than 300 ppm, the standard gaseous ethanol of 300 ppm was selected for the optimization of pH condition of Tris–HCl buffer solution. The highest CL intensity was observed at pH 10.3 (Fig. 3). However, the maximum intensities were higher than 256, could not be detected accurately by the CCD camera (8 bit) at pH 10.3 and pH 10.2. And in order to enhance the sensitivity of this system, Tris–HCl buffer solution (0.1 mol L^{-1}, pH 10.1 not 9.0) was selected and used for further investigations on standard gaseous ethanol and expired gaseous ethanol measurement.

3.3. Standard gaseous ethanol measurement

Under the optimum conditions of 5.0 mmol L^{-1} luminol solution and Tris–HCl buffer solution (0.1 mol L^{-1}, pH 10.1), the temporal images of CL after loading a standard gaseous ethanol (300 ppm) are illustrated in Fig. 4. The upper figures were processed showing the different information of CL generated by the catalytic reaction of ethanol in 3D profile. The lower figures were the images of CL, which processed showing the intensity. As the images (uppers and lowers) shown in Fig. 4, the gaseous ethanol was soluble in Tris–HCl buffer solution gradually, catalyzed by AOD with the production of H_2O_2. And then the CL generated by catalytic reaction of HRP was detected by the CCD camera. Thus there was a delay between the beginning of loading gaseous ethanol and the beginning of the CL. Both of the uppers and the lowers show the image of temporal changes of CL monitored by this system.

The temporal changes of various concentrations of standard gaseous ethanol are shown in Fig. 5 with the images of maximum intensity processed. As figure indicates, the CL intensities increased rapidly following the load of standard gaseous ethanol. The peaks appeared within 90 s and faded away in 200 s. And the image showed that the area became bigger as a result of increment in concentration of gaseous ethanol. The development of this system showed a rapidly and accurately responses and a visible measurement, which could lead expired air analysis to diagnosing and monitoring disease states specifically at real time.

Fig. 6 shows the calibration curve of this system for gaseous ethanol measurement. The CL intensities detected by this system were related to the concentrations of gaseous ethanol from 30 to 400 ppm, as shown as Eq. (1):

$$\text{intensity} = -4.283 + 0.112 \times [\text{gaseous ethanol (ppm)}]$$

where a correlation coefficient of 0.997 for $n = 5$. The calibration range covered the expired gaseous ethanol concentration after oral administration [31]. The maximum intensity of 450 and 500 ppm was too high (higher than 256) to be accurately measured. 450 ppm was the measurement limit under the condition of pH 10.1.The linear range could be broadened out under the other condition of buffer solution pH, if the sensitivity such as a determination limit over 400 ppm was necessary.

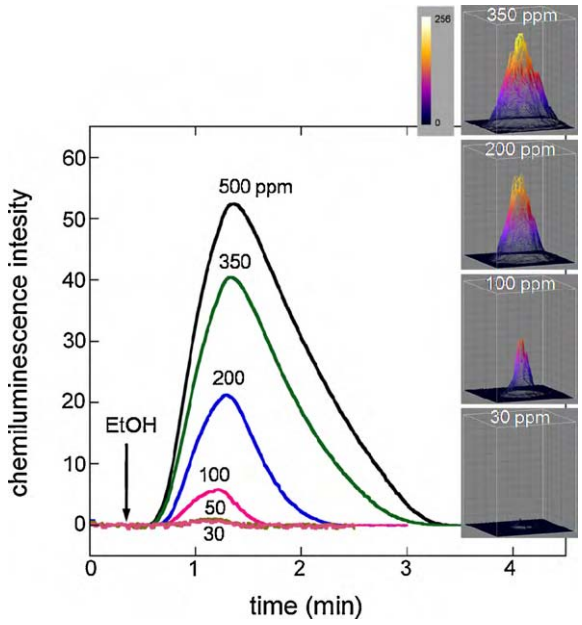

Fig. 5. Temporal changes of various concentrations of standard gaseous ethanol. The CL intensities increased rapidly following the load of standard gaseous ethanol. The peaks appeared within 90 s and faded away in 200 s. And the images showed that the area and the intensity became bigger as a result of increment in concentration of gaseous ethanol. This system showed a rapid and accurate responses and a visible measurement.

The selectivity of this system is shown in Fig. 7. Compared with other chemical substances (2-propanol, methyl ethylketone, acetone, *n*-hexane and *n*-pentane), AOD showed the most activity with ethanol, which is depended on the substrate properties of AOD, and the activity decreases as high molecular weight alcohols and the activity decreases as high molecular weight alcohols. It is able to detect the very component selectively, from more than 200 components.

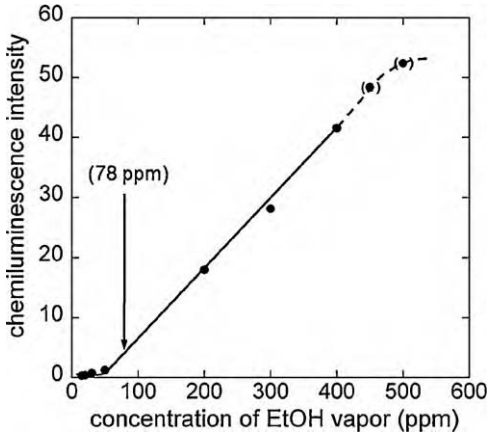

Fig. 6. Calibration curve of this system for standard gaseous ethanol with a correlation coefficient of 0.997, related to the concentration of gaseous ethanol from 30 to 400 ppm for $n = 5$. The maximum intensity of 450 and 500 ppm was too high (higher than 256) to be accurately measured. 450 ppm was the measurement limit under the condition of pH 10.1; arrowhead: permissible limit level (78 ppm) for driving under the influence of alcohol [32].

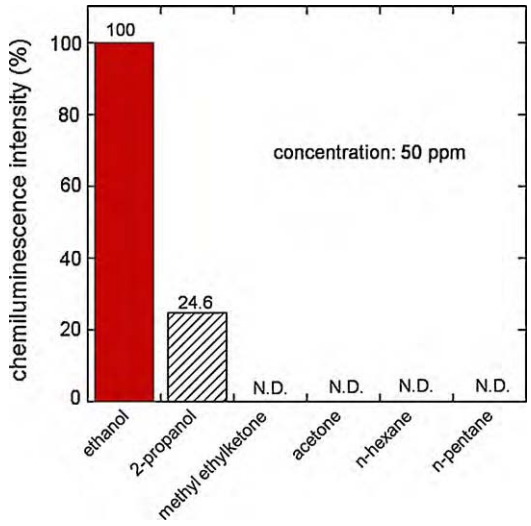

Fig. 7. Selectivity of this system depended on the substrate properties of AOD. Compared with other chemical substances (2-propanol, methyl ethylketone, acetone, *n*-hexane and *n*-pentane), AOD showed the most activity with ethanol and the activity decreases as high molecular weight alcohols.

3.4. Expired gaseous ethanol measurement

Ethanol in expired air after oral administration was selectively detected and measured. Comparison with gas detector tube for ethanol on expired gaseous ethanol concentration value after oral administration is shown in Fig. 8. This system showed a better sensitivity than gas detector tube.

The variation profile of mean of expired gaseous ethanol concentrations for 5 healthy volunteers, who drank an amount of alcohol (0.4 g/kg body weight), is shown in Fig. 9. The expired gaseous ethanol concentration rapidly increased after oral administration. The peaks appeared within 30 min after oral administration and then gradually decreased until the end of sample collection at 2 h. During the first 30 min, the time variation profile based on mean values showed the absorption and distribution function after oral administration, and the values onward showed the elimination function. The absorption and distribution of ethanol in 5 volunteers following first-order absorption process were faster than the elimination process. The differences of the values during the absorption and distribution may be caused by different body compartments. The line illustrates the regression line based on data points from 90 min and onward according to zero-order kinetics for the time variation profile.

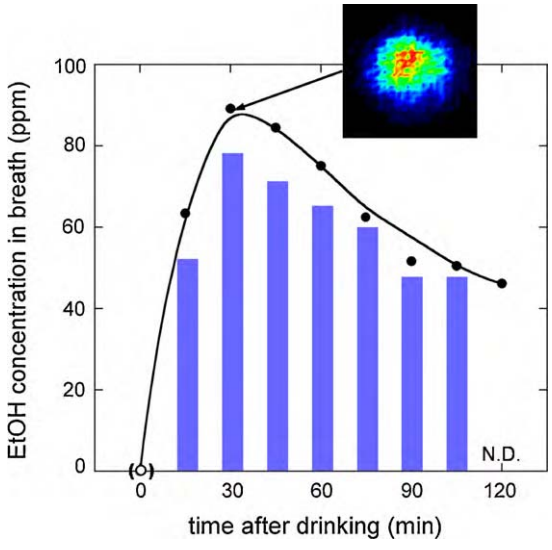

Fig. 8. Comparison of the ethanol concentration changes with time in expired air between this system (●) and the gas detector tube for ethanol (■). This system showed a better sensitivity than gas detector tube.

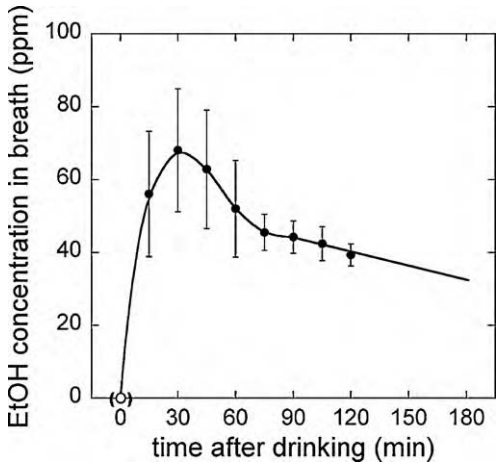

Fig. 9. Time variation profile of mean expired gaseous ethanol concentration. 5 healthy volunteers, 3 males and 2 females, aged from 20 to 30 years, have a body length between 150 and 170 cm and a body weight between 50 and 80 kg. All volunteers, after fasting for at least 4 h, drank beer (0.4 g/kg body weight) during 15 min. All volunteers remained in a chair for the duration of collecting expired air samples. The line illustrates the regression line based on data points from 90 min and onward according to zero-order kinetics for the time variation profile.

This system showed a good sensitivity on expired gaseous ethanol alcohol metabolism-dependence in the liver. Expired gaseous ethanol concentration curves obtained from this system for expired air analysis described in this study indicate a similar tendency to other results reported [31,33]. Expired air analysis would be used in medical diagnosis, because of increased concentrations of some compounds have been shown to correlate with diseases [34,35], such as for the purpose of early cancer diagnosis. And for the advantage of rapid measurement, this system should be used in expired air analysis at real time. In this paper, in order to measure the highest expired gaseous ethanol concentration after ethanol oral administration, pH 10.1 was selected. For the measurement of VOCs in expired air, the sensitivity of this system could be improved by setting pH of Tris–HCl buffer solution higher than 10.1 and/or employing some CL sensitizer.

4. Conclusions

A 2D spatiotemporal visualization system of expired gaseous ethanol after oral administration for real-time illustrated analysis of alcohol metabolism was developed for biomedical applications. Considering the rapid and accurate measurement, a novel HRP–luminol–H_2O_2 based CL measurement system was utilized. The low light CCD camera was first constructed with AOD/HRP-immobilized substrate. The experimental results showed that pH value of Tris–HCl buffer solution played more important role for CL intensity than the catalytic reaction of both AOD and HRP. The advantage of employing a low light CCD camera is that able to record the spatiotemporal change of gaseous ethanol at real time. The calibration range of the visualization measurement was 30–400 ppm for standard gaseous ethanol and the correlation coefficient was 0.997. This system was then used for expired gaseous ethanol measurement, competitive in compare with ethanol detector tube. This system showed good performance in standard gaseous ethanol and expired gaseous ethanol measurement: rapid response, high sensitivity. Moreover, this system

for expired gaseous ethanol concentration value can be adapted to other expired air analysis by varying the enzyme for clinical purpose.

Acknowledgments

This work is partly supported by Japan Society for the Promotion of Science (JSPS) Grants-in-Aid for Scientific Research System, by Japan Science and Technology Agency (JST) and by MEXT (Ministry of Education, Culture, Sports, Science and Technology) Special Funds for Education and Research "Advanced Research Program in Sensing Biology".

References

[1] J.G. Wagner, Pharm. Ther. 12 (1981) 537–562.
[2] W. Miekisch, J.K. Schubert, G.F. Noeldge-Schomburg, Clin. Chim. Acta 347 (2004) 25–39.
[3] M. Phillips, J. Herrera, S. Krishnan, M. Zain, J. Greenberg, R. Cataneo, J. Chromatogr. B: Biomed. Appl. 729 (1999) 75–88.
[4] J.K. Schubert, W. Miekisch, K. Geiger, G.F. Noldge-Schomburg, Expert Rev. Mol. Diagn. 4 (2004) 619–629.
[5] R. Mukhopadhyay, Anal. Chem. 76 (2004) 273A–276A.
[6] A.W. Jones, L. Andersson, J. Forensic Sci. 41 (1996) 916–921.
[7] R.G. Hahn, A. Norberg, A.W. Jones, Am. J. Ther. 2 (1995) 50–56.
[8] K.M. Dubowskl, Clin. Chem. 20/8 (1974) 966–972.
[9] M. Antony, Clin. Chem. 29/1 (1983) 5–15.
[10] L. Pauling, A.B. Robinson, R. Teranishi, P. Cary, Proc. Natl. Acad. Sci. U.S.A. 68 (1971) 2374–2376.
[11] K. Mitsubayashi, H. Matsunaga, G. Nishio, S. Toda, Y. Nakanishi, Biosens. Bioelectron. 20 (2005) 1573–1579.
[12] K. Mitsubayashi, G. Nishio, M. Sawai, T. Saito, H. Kudo, H. Saito, K. Otsuka, T. Noguer, J.-L. Marty, Sens. Actuators B130 (2008) 32–37.
[13] H. Kudo, M. Sawai, X. Wang, T. Gessei, T. Koshida, K. Miyajima, H. Saito, K. Mitsubayashi, Sens. Actuators B141 (2009) 20–25.
[14] F. Wen, S.C. Zhang, N. Na, Y.Y. Wu, X.R. Zhang, Sens. Actuators B141 (2009) 168–173.
[15] L. Wu, J.P. Lei, X.J. Zhang, H.X. Ju, Biosens. Bioelectron. 24 (2008) 644–649.
[16] L.N. Wu, M. McIntosh, X.J. Zhang, H.X. Ju, Talanta 74 (2007) 387–392.
[17] J.P. Gisbert, J.M. Pajares, Aliment Pharmacol. Ther. 20 (2004) 1001–1017.
[18] J. Romagnuolo, D. Schiller, R.J. Bailey, Am. J. Gastroenterol. 97 (2002) 1113–1126.
[19] P.P.R. Rosias, E. Dompeling, M.A. Dentener, H.J. Pennings, H.J.E. Hendriks, M.P.A. Van Iersel, Pediatr. Pulmonol. 38 (2004) 107–114.
[20] M. Phillips, Anal. Biochem. 247 (1997) 272–278.
[21] L. Philipp, B. Florian, R. Josef, Int. J. Mass Spectrom. 239 (2004) 221–226.
[22] S.A. Kharitonov, D.H. Yates, P.J. Barnes, Am. J. Respir. Crit. Care Med. 153 (1996) 454–457.
[23] T.J. Warke, P.S. Fitch, V. Brown, R. Taylor, J.D. Lyons, M. Ennis, M.D. Shields, Thorax 57 (2002) 383–387.
[24] T.B. Xin, S.X. Liang, X. Wang, H. Li, J.M. Lin, Anal. Chim. Acta 627 (2008) 277–284.
[25] S.S. Zhang, Y.M. Yan, S. Bi, Anal. Chem. 81 (2009) 8695–8701.
[26] F. Garcia Sanchez, A. Navas Diaz, C. Delgado Tellez, M. Algarra, Talanta 77 (2008) 294–297.
[27] I.Y. Sakharov, A.N. Berlina, A.V. Zherdev, B.B. Dzantiev, J. Agric. Food Chem. 58 (2010) 3284–3289.
[28] C.V. Popa, A.F. Danet, S. Jipa, T. Zaharescu, Rev. Chim. 61 (2010) 11–16.
[29] L.J. Kricka, R.A.W. Stott, G.H.G. Thorpe, in: W.R.G. Baeyens, D.D. Keukeleire, K. Korkidis (Eds.), Luminescence Techniques in Chemical and Biochemical Analysis, Marcel Dekker, New York, 1991, p. 599.
[30] M. Hnaien, F. Lagarde, N. Jaffrezic-Renault, Talanta 81 (2010) 222–227.
[31] L. Lindberg, S. Brauer, P. Wollmer, L. Goldberg, A.W. Jones, S.G. Olsson, Forensic Sci. Int. 168 (2007) 200–207.
[32] Japan Environmental and Sanitary Center Ed., 1980. A report of chemical malodor analysis. A Study for the Japan Environmental Agency, pp. 248–250.
[33] A.W. Jones, L. Andersson, Forensic Sci. Int. 132 (2003) 18–25.
[34] G. Song, T. Qin, H. Liu, G.B. Xu, Y.Y. Pan, F.X. Xiong, K.S. Gu, G.P. Sun, Z.D. Chen, Lung Cancer 67 (2010) 227–231.
[35] B.J. Novak, D.R. Blake, S. Meinardi, Proc. Natl. Acad. Sci. U.S.A. 104 (2007) 15613–15618.